Tracking the Heat: Temporal Trends in Atlantic Ocean Heat Content and Storm Events

Veronica Patterson

Abstract

This study examines trends in ocean heat content (OHC) in the Atlantic Ocean at the 0–700 meter layer using monthly data spanning 2005 to 2024. The analysis employs regression techniques, beginning with cubic and penalized smoothing splines to capture long-term trends in OHC. Results indicate a consistent increase in OHC over time, reflecting broader patterns of ocean warming. Additionally, the study focuses on OHC during periods corresponding to hurricanes and tropical storms in the Atlantic Basin, analyzing whether similar trends persist under these extreme weather events. The findings reveal that storm events may align with specific fluctuations in OHC, though the broader warming trend persists. These insights contribute to understanding the relationship between ocean heat dynamics and time, offering implications for future studies on ocean warming and extreme weather events.

1 Introduction

Global warming, driven by the long-term heating of the Earth's surface due to human activities such as fossil fuel combustion, has led to increased levels of greenhouse gases that trap heat in the atmosphere [NASA, a]. A significant portion of this excess heat is absorbed by the world's oceans, making OHC a critical indicator for understanding the impacts of climate change on the Earth's energy balance [ECCO]. Ocean water absorbs solar energy, and the upper few meters store more energy than the entire Earth's atmosphere [Dahlman and Lindsey, 2020]. As a result, OHC is measured in units of 10^{22} joules, approximately 17 times the total energy consumed worldwide each year.

The immense heat capacity of the ocean makes it the dominant reservoir for excess heat in the Earth's climate system. Consequently, more than 90 percent of the warming that has occurred on Earth over the past 50 years has been absorbed by the ocean [Dahlman and Lindsey, 2020]. The heat absorbed by the ocean is redistributed, eventually returning to the Earth's system through processes like ice shelf melting, water evaporation, or directly reheating the atmosphere. When the ocean absorbs more heat than it releases over a specific period, its overall heat content increases. [Dahlman and Lindsey, 2020].

The impacts of the rises in OHC are severe and extensive, encompassing rising sea levels, intensified storms, disruptions to marine ecosystems, and the melting of polar ice [NASA, b]. Although global warming is not completely reversible, it can be mitigated, and a key aspect of our role as statisticians is to gather insights into the current state to inspire and inform decisive action.

2 Data

OHC data collection uses a combination of in situ instruments and satellites. A key tool is the fleet of over 3,000 Argo floats, which drift at various depths and periodically ascend to the surface, recording temperature and salinity data as they rise. By converting temperatures to joules, scientists can compare ocean heat to energy in other parts of Earth's climate system [Dahlman and Lindsey, 2020].

The data for this analysis, provided by, NOAA, the National Centers for Environmental Information, consists of a time series of monthly average heat content measurements for the 0–700 meter layer of the Atlantic Ocean, encompassing the entire Arctic Ocean within this dataset. The data starts in January of 2005, and ends in June of 2024, providing 234 observations of Atlantic Ocean Heat Content (AOHC). Additionally, hurricane and tropical storm data were obtained from NOAA, focusing on U.S. landfalling tropical storms and hurricanes over the same time period. This dataset includes maximum wind speeds (measured to the nearest 5 knots) for both tropical storms and hurricanes.

3 Methods

3.1 Model 1: Long-Term Trend

The initial analysis focused on examining long-term trends in AOHC over time. A penalized cubic smoothing spline was fit to time with 55 basis functions. Penalized cubic smoothing splines are well-suited for modeling nonlinear trends over time because they provide a flexible framework to capture gradual changes in the data. The penalty on the second derivative of the spline helps to avoid overfitting by smoothing excessive curvature in the trend, ensuring the model reflects meaningful long-term patterns rather than noise. Additionally, constraints at the boundaries ensure stability at the edges, where extrapolation can often lead to erratic behavior.

The number of basis functions was chosen to balance smoothness and model fit. Through iterative exploration, an optimal configuration was identified that preserved key features of the AOHC trend while avoiding excessive overfitting. This approach allowed the spline to capture the nuanced changes in AOHC over time, providing insights into its long-term behavior.

3.2 Model 2: Short-Term Variations

To account for short-term variations in AOHC, a second model was developed by introducing an additive structure. This included:

1. A penalized cubic smoothing spline with 45 basis functions for the overall temporal trend.
2. A second smoothing spline with 12 basis functions for the months, modeled with a cyclic basis function to capture seasonality across the calendar year.

Despite this improvement, model diagnostics indicated the presence of residual autocorrelation.

3.3 Model 3: AR(1)

To address residual autocorrelation, a final additive smoothing spline model was fit. The components included:

1. A penalized cubic smoothing spline with 45 basis functions for the overall time trend.
2. A cyclic smoothing spline for seasonality, refined to use 8 basis functions (2 basis functions per season, reflecting four seasons per year).

An autoregressive AR(1) structure was incorporated to effectively model temporal autocorrelation in the residuals. The AR(1) structure accounted for dependencies between successive observations, with each observation being influenced by its nearest neighbor in time. This final model with the AR(1) structure successfully removed residual autocorrelation while balancing the flexibility of the smooth term for time and seasonality. The combination of these components provided a robust framework for analyzing AOHC trends over time.

3.4 Model 4: Storm-Specific AOHC

To examine the relationship between AOHC and hurricane or tropical storm activity, a fourth model was developed. Using NOAA data, AOHC observations corresponding to months and years when a hurricane or tropical storm occurred in the Atlantic basin from 2005 to 2024 were identified, resulting in 85 observations of AOHC during storm events.

A Gamma Generalized Linear Model (GLM) was used to analyze this data. The model included year, maximum wind speed (measured in knots), and storm type (tropical storm or hurricane) as predictors. An additive model was chosen due to the insignificance of interaction terms. This approach allowed for the investigation of storm-specific AOHC and its relationship with time and storm characteristics.

4 Results

4.1 Model 1: Long-Term Trend

Findings

Model 1 revealed an increase in AOHC from 2005 to 2024, indicative of a warming trend in the Atlantic Ocean at the 0-700 meter layer. This increase aligns with broader patterns of ocean warming observed in recent decades.

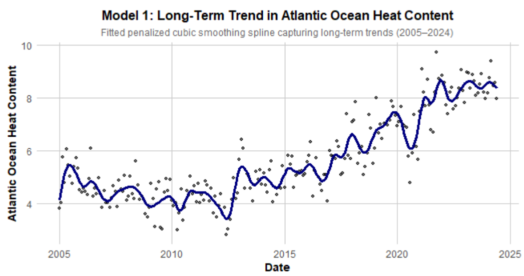

Figure 1: Model 1: Long-Term Trend.

Model Diagnostics

While the model effectively captured the long-term trend, residual diagnostics indicated temporal autocorrelation in the model's errors. The autocorrelation function (ACF) plot in the Appendix (Figure 6) shows this pattern of correlation between residuals over successive time steps. This suggests that the model did not fully account for temporal dependencies, necessitating further refinement.

4.2 Model 2: Short-Term Variations

Findings

Model 2 revealed both long-term and monthly variations in Atlantic Ocean Heat Content (AOHC) from 2005 to 2024. The penalized cubic smoothing spline for time captured a steady increase in AOHC, as in Model 1. The addition of a cyclic smoothing spline for months highlighted seasonal fluctuations, with notable peaks and troughs recurring annually. The observed seasonal cycle likely reflects natural variability in ocean heat dynamics driven by atmospheric and oceanographic processes.

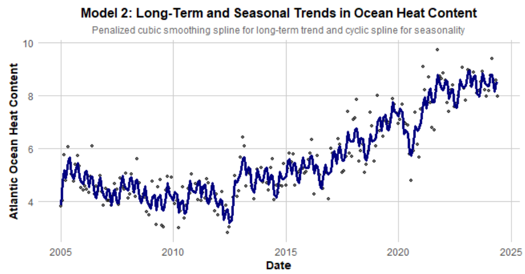

Figure 2: Model 2: Short-Term Variations.

Model Diagnostics

While the autocorrelation in the residuals decreased significantly compared to Model 1, residual diagnostics still indicated some temporal autocorrelation (Appendix, Figure 7), suggesting further refinement was needed to fully account for dependencies in the data.

4.3 Model 3: AR(1)

Findings

Model 3 effectively captured both the long-term trend and seasonal variability in AOHC from 2005 to 2024. The inclusion of an AR(1) structure successfully addressed residual autocorrelation observed in previous models, allowing the smooth terms for time and seasonality to focus on broader patterns in the data.

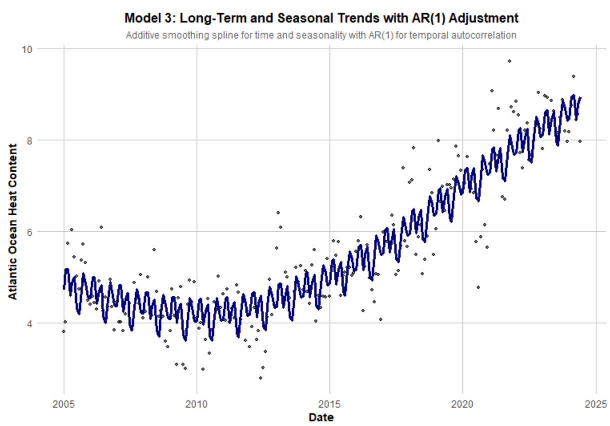

Figure 3: Model 3: AR(1).

Figure 4 below displays the fitted smooth terms for the AR(1)-adjusted model, capturing both the long-term trend and seasonal variation in AOHC. The solid lines represent the estimated smooth functions, while the dashed lines denote the approximate 95% confidence intervals.

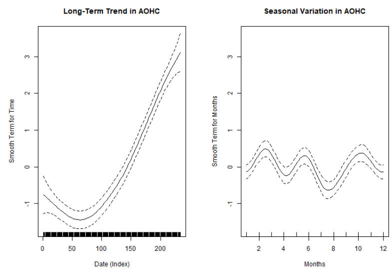

Figure 4: Smoothing Terms for AR(1) Model.

- **Long-Term Trend (Left Panel):** The smooth term for time indicates a clear and nonlinear upward trend in AOHC, suggesting a steady increase from the 2010's to 2024. This trend reflects long-term ocean warming. The steepening of the curve in recent years suggests an acceleration in warming rates.

  For interpretability purposes, Date Index (x-axis) 1 corresponds to January 2005, 50 corresponds to February 2009, 100 to April 2013, 150 to June 2017, and 200 to August 2021.

- **Seasonality (Right Panel):** The smooth term for months in reveals a multi-modal seasonal pattern in AOHC. Three distinct peaks are observed:

  - **Early Spring (March):** A small peak in AOHC is observed during early spring. This corresponds to the recovery of ocean heat content after winter, as increasing solar radiation begins to warm the surface waters [Roemmich and Gilson, 2009].
  - **Early Summer (June):** A second peak occurs in early summer, reflecting the effect of strong solar heating and rising atmospheric temperatures. This marks a period of significant heat absorption by the ocean's upper layers [Trenberth et al., 2011].
  - **Late Fall (October-November):** The last peak is observed in late fall. By this time, the ocean has accumulated heat over the summer months, reaching its maximum heat content before cooling processes dominate in winter [Levitus et al., 2012].

This pattern reflects the ocean's thermal inertia, highlighting AOHC's ability to absorb, store, and redistribute heat. Seasonal fluctuations are driven by surface heating, wind-driven mixing, and currents, resulting in the observed multi-modal pattern [Trenberth et al., 2011].

It's important to note that while the amplitude and phase of seasonal cycles may remain consistent, as designed by the model, the baseline upon which these cycles operate is rising, leading to higher overall temperatures even during cooler seasons.

Model Diagnostics

To evaluate the performance of the final model, several diagnostic checks were performed.

Autocorrelation

The inclusion of an AR(1) structure successfully addressed the temporal autocorrelation observed in earlier models. This is confirmed by the autocorrelation plot (Appendix, Figure 8), which shows that the residuals exhibit no significant temporal dependency.

Residual Analysis

Residual diagnostics indicate that the residuals are appropriately centered around zero and show no discernible patterns or heteroscedasticity (Appendix, Figure 9). Additionally, a normality plot (Appendix, Figure 10) suggests that the residuals are approximately normally distributed, supporting the adequacy of the model.

Effective Degrees of Freedom (EDF)

The effective degrees of freedom (EDF) for the smooth terms provide insight into the model's flexibility:

- **Time:** The EDF for the smooth term of time is 4.33, reflecting the model's ability to capture long-term trends without overfitting. Given the inclusion of the AR(1) structure, it is expected that the EDF for time is relatively low, as the AR(1) term captures much of the temporal autocorrelation.
- **Months:** The EDF for the smooth term of months is 5.75, indicating sufficient flexibility to capture the seasonal variability in AOHC while avoiding overfitting.

Adjusted R^2

The adjusted R^2 value for the final model is 0.856, indicating that the model explains 85.6% of the variability in AOHC. This high value reflects the strong overall performance of the model in capturing both long-term trends and seasonal patterns.

Conclusion

The diagnostic checks confirm that the final model is well-suited for the data. The AR(1) structure eliminated residual autocorrelation, while the smooth terms effectively captured the underlying patterns in AOHC. Combined with the high adjusted R^2, these results demonstrate the robustness and reliability of the model.

4.4 Model 4: Storm-Specific AOHC

For Model 4, 84 AOHC data points corresponding to hurricanes or tropical storms were analyzed over time using a Gamma GLM with a log link function. The model analyzes AOHC as a function of three predictors:

- **Year:** A categorical predictor with 2005 as the baseline year.
- **Max Wind Speed:** A continuous predictor representing the maximum wind speed of the storm (in knots).
- **Tropical Storm or Hurricane:** A categorical predictor indicating whether the data point corresponds to a tropical storm or a hurricane, with hurricane as the baseline category.

Model Rationale

A Gamma distribution with a log link was chosen due to the right-skewed nature of the data and the non-negativity of AOHC values, as observed in its kernel density estimate (KDE). An additive model was selected because interaction terms were found to be statistically insignificant during exploratory analysis. The model coefficients and p-values are provided in the Appendix (Table 1). Because of the log link, the coefficients represent changes in the logarithm of the expected AOHC. Negative coefficients indicate a decrease in AOHC compared to the baseline, with the magnitude of the decrease expressed as a percentage when the coefficient is exponentiated. Positive coefficients indicate an increase in AOHC compared to the baseline, with the magnitude of the increase expressed as a percentage when exponentiated.

Findings

- **Significance of Predictors:**
  - **Year:** The coefficients for the categorical variable Year indicated a clear pattern. Years prior to 2017 had negative coefficients relative to the baseline year (2005), while years after 2017 exhibited positive coefficients. Interpreted on the response scale (due to the log link function), this suggests a shift in AOHC trends during storm events around this period, with a transition from lower AOHC in earlier years to higher AOHC in more recent years.
  - **Max Wind Speed:** The coefficient for maximum wind speed during hurricanes and tropical storms was insignificant but exhibited a negative slope. On the response scale, this indicates that higher wind speeds were associated with slightly lower predicted AOHC, although the effect was not statistically significant. This finding is intriguing though, as it aligns with studies suggesting that during La Niña events, reduced vertical wind shear over the Atlantic Ocean, driven by cooler sea surface temperatures in the central and eastern Pacific Ocean, can influence storm dynamics [Florida Oceanographic Society, 2024].
  - **Tropical Storm or Hurricane:** The categorical variable "Tropical Storm or Hurricane" was also insignificant, indicating no substantial difference in predicted AOHC between tropical storms and hurricanes when accounting for other predictors.

- **Figure Interpretation:** A plot showing the effect of Year on AOHC while holding other variables constant is provided below. This figure highlights the temporal evolution of AOHC during storm events.

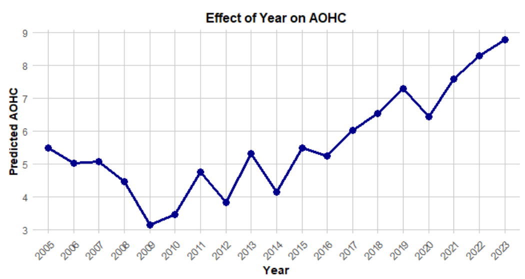

Figure 5: Effect of Year on Storm Event AOHC.

  At the 0.05 significance level, the following years were found to have statistically significant coefficients: 2008, 2009, 2010, 2011, 2012, 2014, 2018, 2019, 2020, 2021, 2022, and 2023.

5 Discussion

The results from Models 1 through 3 consistently demonstrate a clear and significant increase in AOHC over time. By accounting for seasonal variations, models 2 and 3 highlight that this upward trend persists even when considering the cyclic seasonal fluctuations. This finding aligns with the current scientific consensus, as NOAA emphasizes that the ocean is steadily warming. The observed trend is consistent with the notion that global warming is driving long-term increases in ocean heat content.

Historically, the ocean has cycled between hotter and cooler periods due to natural variability, such as El Niño and La Niña events. However, recent data suggest that the cooler periods are occurring less frequently and with reduced intensity. The most recent El Niño event officially ended in May 2024. As noted by Yale Climate Connections, "In theory, the transition out of a strong El Niño should begin to cool the Atlantic to levels more in line with the current trajectory of global warming. So far, this hasn't happened" [Lowry, 2024]. This observation underscores the unprecedented nature of the current warming trend and its potential departure from historical patterns.

The findings from Model 4 provide additional insights into AOHC trends during tropical storm and hurricane events. While the primary drivers of AOHC variability during these events appear to be effects of time and seasonal fluctuations, the effect of maximum wind speed of the storm events, though insignificant, exhibited a negative slope. This raises intriguing questions about the potential influence of atmospheric dynamics, such as reduced vertical wind shear during La Niña events, on AOHC. Further research could explore these dynamics more deeply.

Additionally, the effect of year on AOHC, as visualized in Figure 5, suggests the possibility of a change point in the trend. Years prior to 2017 were associated with negative coefficients relative to the baseline year (2005), while years after 2017 exhibited positive coefficients, indicating a potential shift in AOHC patterns. Identifying and analyzing such change points in AOHC trends could provide critical insights into the underlying drivers of ocean warming. Notably, NASA states that the warming trend of the entire ocean remained relatively steady from 1992 to 2017 but experienced a marked acceleration from 2017 through May 2024. Understanding the factors driving this recent surge in ocean heat content is currently a key focus of ECCO researchers [ECCO].

Overall, the observed long-term increase in AOHC aligns with predictions of global warming impacts on the ocean. These findings reinforce the urgent need for continued monitoring and modeling of ocean heat content to understand its role in the global climate system and its implications for weather patterns, sea-level rise, and marine ecosystems.

References

LuAnn Dahlman and Rebecca Lindsey. Climate change: Ocean heat content. National Oceanic and Atmospheric Administration, August 2020. URL `https://www.climate.gov/news-features/understanding-climate/climate-change-ocean-heat-content`.

ECCO. Ocean Heat Content. `https://ecco-group.org/ohc/`.

Florida Oceanographic Society. El niño vs. la niña: What's the difference?, 2024. URL `https://www.floridaocean.org/blog/el-nino-vs-la-nina`. Accessed: 2024-11-30.

Sydney Levitus, John I Antonov, Tim Boyer, Olga K Baranova, Hernan E Garcia, Ricardo A Locarnini, Alexey V Mishonov, John R Reagan, Dan Seidov, and Eugene S Yarosh. World ocean heat content and thermosteric sea level change (0–2000 m), 1955–2010. *Geophysical Research Letters*, 39(10), 2012.

Michael Lowry. What you need to know about record-breaking heat in the atlantic, 2024. URL `https://yaleclimateconnections.org`.

NASA. What is Climate Change? `https://science.nasa.gov/climate-change/what-is-climate-change/`, a.

NASA. The Ocean and Climate Change. `https://science.nasa.gov/earth/explore/the-ocean-and-climate-change/`, b.

Dean Roemmich and John Gilson. The 2004–2008 mean and annual cycle of temperature, salinity, and steric height in the global ocean from the argo program. *Progress in Oceanography*, 82(2): 81–100, 2009.

Kevin E Trenberth, John T Fasullo, and Magdalena A Balmaseda. Changes in ocean heat content and heat distribution. *Nature Climate Change*, 1(10):515–518, 2011.

Appendix

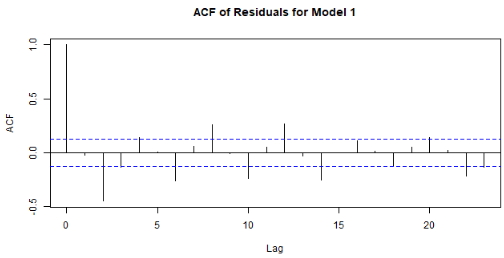

Figure 6: Autocorrelation Funtion (ACF) Plot for Model 1.

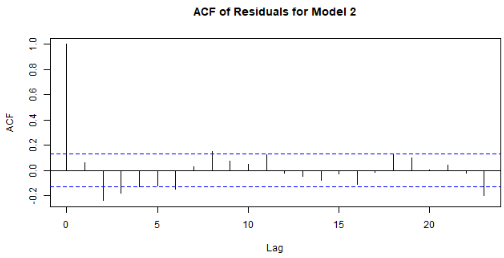

Figure 7: Autocorrelation Funtion (ACF) Plot for Model 2.

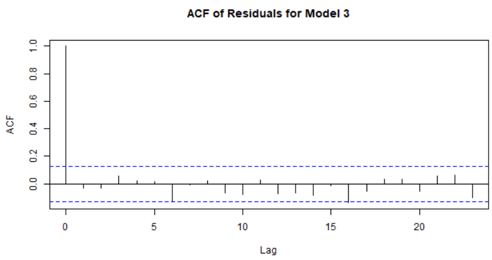

Figure 8: Autocorrelation Funtion (ACF) Plot for Model 3.

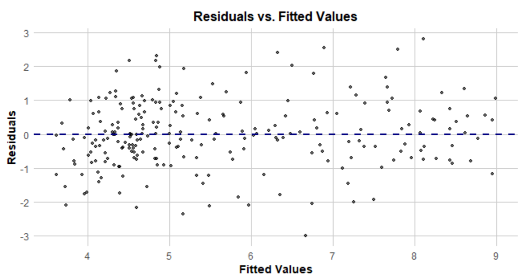

Figure 9: Residuals vs. Fitted Values (Model 3).

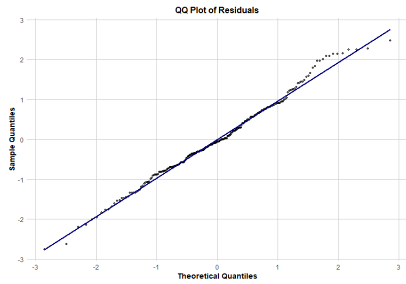

Figure 10: QQ Plot for Normality of Residuals (Model 3).

Predictor	**Log Estimate**	**p-value**
Baseline (Intercept)	1.7842	$<$ 2e-16
Year 2006	-0.0863	0.1951
Year 2007	-0.0781	0.3821
Year 2008	-0.2081	0.0003
Year 2009	-0.5540	2.23e-05
Year 2010	-0.4560	0.0004
Year 2011	-0.1428	0.0427
Year 2012	-0.3576	2.58e-06
Year 2013	-0.0309	0.7992
Year 2014	-0.2815	0.0221
Year 2015	-0.0013	0.9884
Year 2016	-0.0476	0.5338
Year 2017	0.0930	0.0998
Year 2018	0.1756	0.0077
Year 2019	0.2833	0.0004
Year 2020	0.1580	0.0029
Year 2021	0.3234	6.20e-08
Year 2022	0.4112	2.10e-05
Year 2023	0.4692	5.97e-08
Max Wind Speed	-0.0012	0.1820
Tropical Storm	-0.0805	0.1126

Table 1: Coefficients for Model 4